Reprinted from Applied Optics, Vol. *26*, page 3573, September 1, 1987

Double optical resonance mass selective detection of aromatic molecules in a supersonic molecular beam

Jack A. Syage and John E. Wessel

Optical excitation followed by ion mass detection in a supersonic molecular beam can offer unusually high levels of selectivity for detection of trace concentrations of material in the atmosphere. We describe recent work involving two-color excitation of aromatic molecules in a supersonic molecular beam, time-of-flight mass spectrometer. It is shown how double resonance excitation in cold molecules can provide two very selective stages of optical selectivity, further augmented by single mass detection. Three applications are described: (1) Two-color excitation to higher excited electronic states is illustrated for final states above and below the ionization potential. (2) Stimulated emission pumping is shown to allow selective identification using ion dip detection. (3) Resonance ion dissociation is demonstrated as a means for obtaining double optical and double mass selectivity.

I. Introduction

Double resonance excitation in supersonic molecular beams[1–7] has proved to be a very powerful means for studying excited states not accessible by conventional one-photon excitation. The highly selective nature of the excitation process suggests important applications to chemical analysis and trace detection. Very sensitive and selective detection capabilities (part-per-billion detection limits) have recently been demonstrated using single-color resonance ionization in a molecular beam mass spectrometer.[8,9] However, what can ultimately limit the effective sensitivity of any detection device is the selectivity of the method against other molecules in much higher abundance (i.e., the discrimination ratio). The combined optical/mass selectivity involving cold molecules can account for a high level of selectivity.[9]

Fundamental to these studies are the benefits of molecular cooling that occur in a supersonic expansion.[10] The very narrow distribution of initial states is responsible not only for near quantitative excitation with single wavelengths of light but excitation to single discrete levels. This makes possible single vibronic level excitation in excited electronic states as well as formation of rovibrationally cold ions.

The work described demonstrates spectrally selective excitation and fragmentation processes in aromatic hydrocarbons using double resonance excitation/ionization mass spectroscopy. A variety of so-called triply dispersive (two optical and one mass) detection schemes are considered involving final resonance states both above and below the ionization potential. In the latter case, we employ the technique of ion dip detection[3–6,11] to monitor the molecule of interest. In this technique, two-photon resonance ionization (R2PI) through an intermediate state $|1\rangle$ generates an ion mass signal; this signal in turn experiences a decrease when a third photon competes with ionization by resonance excitation from the intermediate state $|1\rangle$ to another state $|n\rangle$. In this manner, we have studied higher excited electronic states reached by the resonant third photon as well as ground vibrational states by stimulated emission pumping. Final resonance states above the ionization potential are also discussed involving discrete vibrational autoionization from Rydberg states. Finally, a method is illustrated for obtaining four stages of selectivity (two optical and two mass). This is achieved by resonance ionization (involving the first laser) and parent ion detection followed by selective resonance ion dissociation (second laser) and fragment ion detection.

II. Experimental

A supersonic molecular beam time-of-flight (TOF) mass spectrometer, depicted in Fig. 1, was used for the

The authors are with Aerospace Corporation, P.O. Box 92957, Los Angeles, California 90009.

Received 27 February 1987.
0003-6935/87/173573-06$02.00/0.

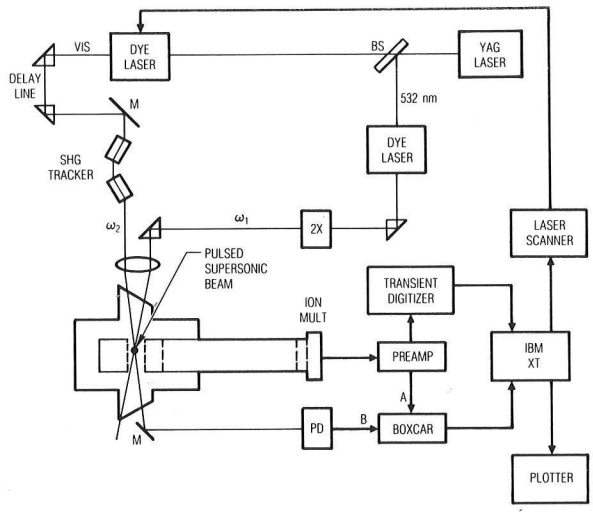

Fig. 1. Schematic of the experimental apparatus. A home-bulit grazing incidence dye laser is used to generate ω_1 (UV) and a commercial scanning dye laser to produce ω_2 (UV and VIS): BS, beam splitter; *M*, mirror; SHG, single harmonic generation; PD, photodiode.

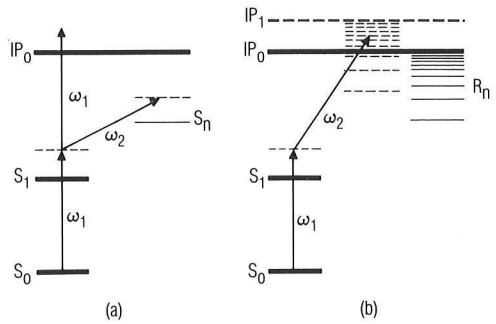

Fig. 2. Double resonance excitation scheme for higher excited electronic state and Rydberg detection: (a) excitation to final states below the ionization potential IP_0 using ion dip detection; (b) excitation to final states above IP_0 that undergo autoionization.

experiments reported here.[6] The vacuum system consists of differentially pumped source and excitation chambers. A third stage of differential pumping was provided at the detector end of the TOF drift tube. A temperature controlled magnetic solenoid pulsed nozzle in the source chamber was used for the supersonic expansion which entered the ionization chamber through a 1-mm skimmer. Ions were accelerated into a zero field drift region of 1-m length, where they were detected by a Johnston multiplier. Space focusing conditions were met by applying extraction and acceleration fields of 200 and 1800 V, respectively, across 1-cm grid spacings. For field sensitive experiments, the extraction field was reduced to 50 V/cm.

Excitation sources consisted of a home-built grazing incidence dye laser which served as the ionizing source ω_1 and a commercial dye laser as the second resonance source ω_2. Pulse durations of both beams are ~5 ns. The amplified fundamental pulse from the grazing incidence laser was 1 mJ or less in energy, the UV beam from this laser was ~20 μJ, and the fundamental from the commercial dye laser had energies typically ranging from 1 to 10 mJ/pulse. The commercial laser beam was either used directly or frequency doubled (25–200 μJ/pulse) and recollimated for UV scans. For visible scans, the pulse energy was controlled by changing the Nd:YAG pump intensity incident on the dye laser with a rotatable halfwave plate. Intensity was monitored with a spectrally flat photodiode or a thermopile based detector. Ultraviolet scans reported in this paper were performed without active control of laser intensity. The ω_1 and ω_2 pulses were focused into the ionization region of the molecular beam by a 30-cm focal length lens. A spherical lens was used for high intensity investigations, and a cylindrical lens was used for routine measurements where minimum power broadening was desired.

Mass spectra were recorded using a 200-MHz transient digitizer. Excitation spectra involving laser wavelength scans were recorded using gated TOF mass detection. Two-photon ionization signals involving the scanning ω_2 laser only were suppressed when necessary by operating a shutter that blocked the ω_1 pulse on alternate triggers and subtracting the ω_2 only signal from the $\omega_1 + \omega_2$ signal.

III. Multiresonant Excitation, Ionization, and Dissociation

A. Excitation of Higher Electronic and Rydberg States

Discrete higher excited electronic states can offer very specific conditions for molecular detection by double resonance excitation. This is particularly true of Rydberg states which tend to have narrow excitation linewidths. We consider excitation to final resonant states below and above the first ionization threshold. The excitation schemes, which involve ion dip and autoionization detection, respectively, are portrayed in Fig. 2.

1. Below Threshold Excitation—Ion Dip Detection

Detection of a higher excited state S_n in aniline and aniline-d_5 is illustrated in Fig. 3 for the excitation scheme found in Fig. 2(a). The aniline S_n spectra were recorded by generating an ion signal by R2PI via the $S_1(\tilde{A}^1B_2) \leftarrow S_0(\tilde{X}^1A_1)0_0^0$ transition ω_1, while a second dye laser ω_2, overlapped and synchronous in time, was tuned through the $S_n(v) \leftarrow S_1(0)$ resonances.[3] These absorptions compete with ionization, thereby creating the ion dip signals. The excitation spectra were mass-selected by gating the aniline parent ion signal M^+.

Spectroscopically, the two-color ion dip technique is important for detecting higher excited electronic states that are too short-lived to be detected by conventional ionization or fluorescence detection methods. In fact, the lifetime of the final state determines in part the strength of the ion dip signal and hence the sensitivity for that particular excitation. For example, saturation of a long-lived state would give a maximum ion dip signal of ~50%. However, if the upper state decays at a rate greater than the ω_2 pumping rate, the lower state can be quantitatively depleted, leading to ion dip signals >50% and hence the potential for

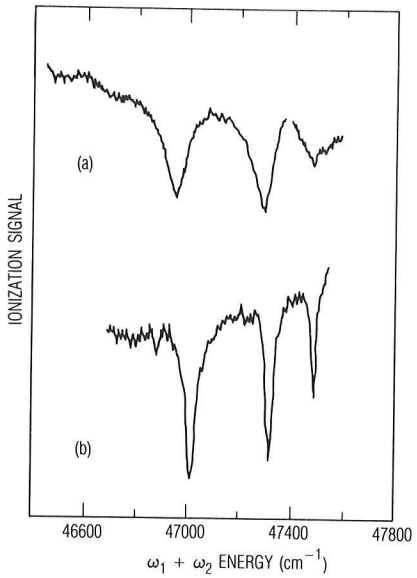

Fig. 3. Ion dip spectrum for the $S_n(v) \leftarrow S_1(v = 0)$ absorption of aniline and aniline-d_5. Ion dip intensities are plotted relative to the ion signal level in the absence of the ω_2 beam.

very sensitive detection. Ion dip signals exceeding 50% were observed for nearly all $S_n(v) \leftarrow S_1(0)$ transitions in aniline and aniline-d_5 by decreasing the ω_1 and increasing the ω_2 intensity. Apparently, the S_n state undergoes rapid decay,[3,12] either by dissociation or radiationless decay to a set of states that are not ionized by ω_1 or ω_2.

It is interesting to note that the spectral linewidths for aniline-d_5 are significantly narrower than for the protiated molecule. This observation may be attributed to the reduction in vibrational frequencies that occurs on deuteration which leads to a weaker coupling between initial and final states due to the larger difference in quantum number. This Franck-Condon effect outweighs the effects of an increased density of states.[13] We have recently obtained evidence for narrower electronic transitions at higher energy which may prove promising from a detection standpoint.

2. *Above Threshold Excitation—Autoionization*

Vibrationally excited Rydberg series converge to the same vibration of the ion and, therefore, account for discrete states above the adiabatic ionization threshold IP_0 [Fig. 2(b)]. These states undergo vibrational autoionization due to their interaction with the ionization continua associated with the zero-point vibrational level or other low energy vibrational ionization thresholds. The interactions are often sufficiently weak that transitions to these states can be rather sharp. An example of excitation to discrete states above IP_0 is given in Fig. 4 for naphthalene and naphthalene-d_8. The ω_1 laser excites a specific vibrational level in S_1; the ω_2 laser then excites a Rydberg state with the same vibration via an efficient ν_1^1-type excitation. Often many members of an autoionizing Rydberg series can be identified[7] providing additional possibilities for selective detection. The linewidths for

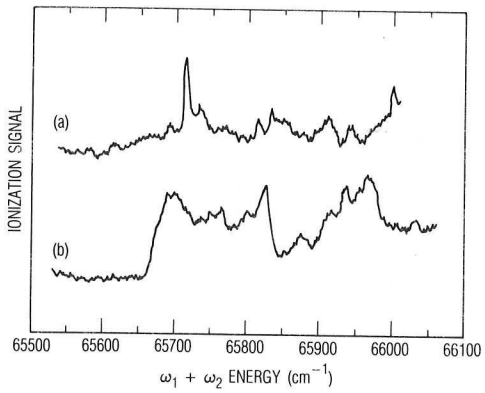

Fig. 4. Autoionization spectra of vibrational Rydberg states for (a) naphthalene-d_8 and (b) naphthalene-h_8. Excitation was via the intermediate state $S_1(\nu_7)$ (i.e., 7^1) in both cases. The ionization step at 65,665 cm^{-1} in (b) is due to IP_0.

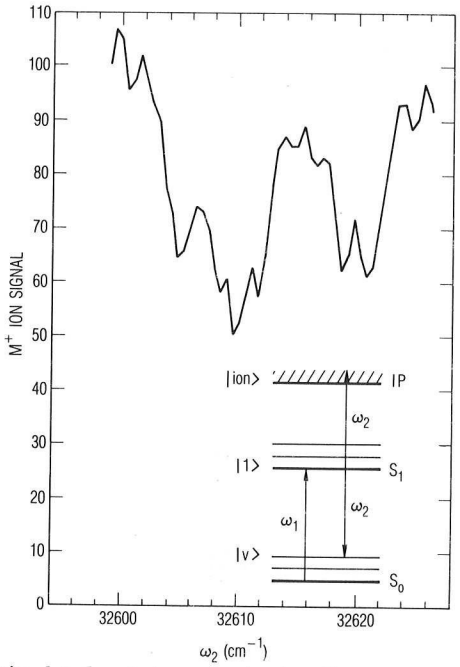

Fig. 5. Stimulated emission pumping ion dip spectrum of aniline. The delayed ω_2 ionizing pulse produces downward transitions when tuned into resonance, thereby generating an ion dip. The SEP transitions are tentatively assigned to the S_0 vibrational levels, 8_1 and 12_16a_1, at 1420 and 1432 cm^{-1}, respectively.

the autoionizing transitions are significantly narrower on deuteration of naphthalene, a trend also observed for aniline above.

B. Stimulated Emission Pumping

Stimulated emission pumping (SEP) is particularly suitable for selective detection since the final resonance state, usually a vibration in the ground electronic state, is typically a narrow transition and spectroscopically well characterized. A SEP spectrum is illustrated for aniline along with the excitation scheme in Fig. 5. Since ω_2 is primarily responsible for ionization and down-pumping, the conditions for spatial and

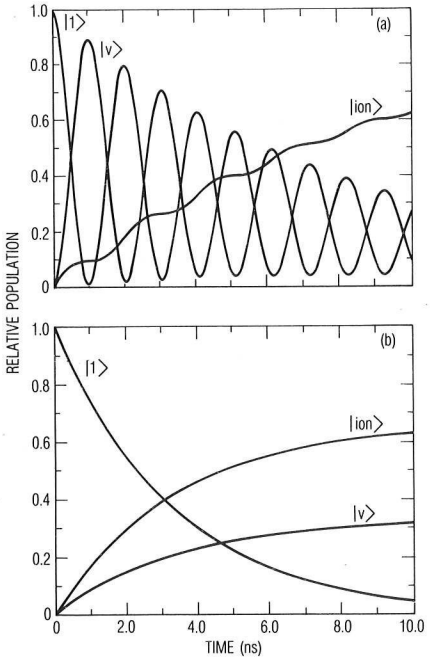

Fig. 6. Calculated relative populations of the initially excited $S_1(v = 0)$ state $|1\rangle$, the down-pumped $S_0(v)$ state $|v\rangle$, and the ion state $|\text{ion}\rangle$ as a function of laser power and pulse duration: (a) strong pumping, $\Omega = 2 \times 10^9\ s^{-1}$, and (b) weak pumping, $\Omega = 2 \times 10^7\ s^{-1}$.

temporal beam alignment are somewhat less stringent than for other excitation conditions described in this paper.

SEP using ion dip detection was previously observed by Murakami *et al.*[4] for aniline. Using a 3-cm^{-1} bandwidth dye laser, they observed ion dip signals that could be modeled using an incoherent kinetic model for laser pump energy dependence. In our studies, using 0.5- and 0.05-cm^{-1} bandwidth down-pumping excitation, we observed SEP ion dip intensities that deviated significantly from the predictions of a simple kinetic model and in fact observed on occasions the disappearance of the SEP signals at higher powers. The narrower bandwidth excitation employed in our work contributed to a higher effective peak power. Consequently, the different behavior we observed, compared to the work of Murakami *et al.*, simply reflects the low power and high power limits of coherent excitation.

We examine the effect of coherent excitation by intense laser pulses using a simple density matrix model. The model assumes coherent pumping of a two-level system where one of the levels may also be pumped to an irreversible third state (i.e., the ion) by the same excitation source (Fig. 5). The equations of motion[14] are given by

$$\dot{\rho}_{11} = +\frac{1}{2} i\Omega(\rho_{12} - \rho_{21}) - \frac{\rho_{11}}{\tau} - R\rho_{11}, \tag{1}$$

$$\dot{\rho}_{22} = -\frac{1}{2} i\Omega(\rho_{12} - \rho_{21}) + \frac{\rho_{11}}{\tau}, \tag{2}$$

$$\dot{\rho}_{33} = R\rho_{11}, \tag{3}$$

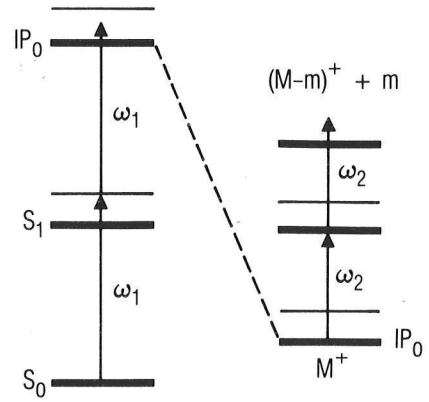

Fig. 7. Excitation and detection sequence for resonance ion dissociation.

$$\dot{\rho}_{21} = -i\Delta\rho_{21} - \frac{1}{2}\left(\frac{1}{\tau} + \frac{1}{T_I} + R\right)\rho_{21} - \frac{1}{2} i\Omega(\rho_{11} - \rho_{22}), \tag{4}$$

where Δ is the detuning frequency, Ω the Rabi frequency of the $|1\rangle \rightarrow |2\rangle$ transition, $1/\tau$ the spontaneous emission rate, R the ionization rate, and $1/T_I$ the dephasing rate of the coherent pumping. We have not considered laser pulse inhomogeneities or off-resonance excitation due to Doppler widths or rotational contours. Here we assign $|2\rangle$ to the $S_0(v)$ down-pumped state which we label $|v\rangle$ and $|3\rangle$ to the ion which is formed irreversibly. Figure 6 illustrates the evolution of population for weak vs strong pumping as a function of pulse duration. At high power, a coherent oscillation in the populations of $|1\rangle$ and $|v\rangle$ occurs (i.e., Rabi nutation), which results in an oscillation in the ratio $|v\rangle/|\text{ion}\rangle$ and, therefore, the ion dip signal as well [Fig. 4(a)]. For weak excitation, one finds that $|v\rangle/|\text{ion}\rangle$ is essentially constant over the duration of the driving field [Fig. 4(b)] and is, therefore, describable by kinetic equations of the type derived by Murakami *et al.*[4] For maximum detection efficiency, one should seek the combination of power and pulse duration that gives the maximum down-pumping (so called π pulse). Additional power in these conditions acts to decrease the SEP ion dip signal, although some oscillatory behavior may persist. The oscillations should actually be more damped when account is taken of laser pulse inhomogeneities and temporal profile as well as the rotational contour of the transition.

C. Resonance Ion Dissociation in Naphthalene Ions

We have been investigating the potential for obtaining double mass selectivity along with the usual double optical selectivity made possible by two-color excitation. The method involves resonance ion dissociation (RID); the excitation sequence is illustrated in Fig. 7. In this scheme, the first laser populates a single vibrational level of the ion by R2PI, and the second laser dissociates the ion by resonance enhanced multiphoton dissociation. The dissociation process is evident by observing a decrease in the parent ion M^+ signal (i.e., ion dip) and a corresponding increase in the fragment ion $[M - m]^+$ signal. Detection of both the

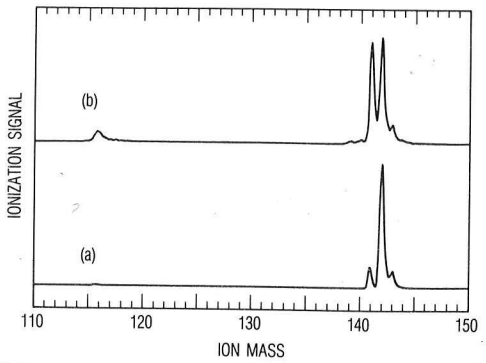

Fig. 8. Mass spectra of 2-methylnaphthalene showing resonance ion dissociation: (a) R2PI by ω_1 only at 308.3 nm; (b) R2PI by ω_1 and RID by ω_2 at 662 nm revealing an efficient and specific H atom dissociation.

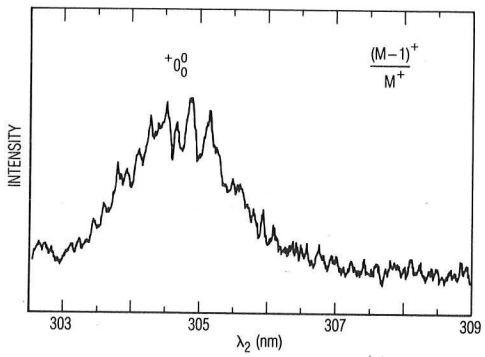

Fig. 9. RID fragment ion formation spectra from vibrationless $^{+}0_0$ cations formed by ω_1 R2PI excitation at 302.98 nm. H atom loss channel is monitored by the ratio $[M-1]^+/M^+$.

parent ion and the characteristic fragment ion, therefore, may hold promise as a very selective detection method.

Singly charged cations of aromatics have been studied in a variety of low temperature matrices.[15] The vibrationally resolved ion spectra are distinctive, showing strong red absorption bands corresponding to transitions between normally filled molecular orbitals in the neutral. Low pressure vapor phase studies of the spectroscopy of ions formed by electron impact in an ICR spectrometer[16] and by MPI in a mass spectrometer,[17] however, failed to reveal the vibrational structure that was evident in the low temperature matrix spectra.[15] This may be attributed to the thermal energy content of the precursor neutral molecules. By cooling the precursor molecules by supersonic expansion, one may expect to form cold ions by R2PI.

We observed vibrationally resolved resonances in naphthalene and 2-methylnaphthalene (2-MeN) by recording RID spectra following selective vibronic preparation of the molecular cation.[6] These studies focused on the low energy H atom photodissociation channel of naphthalene and 2-MeN cations as a probe of resonant absorption by the molecular ion (Fig. 7). For the 2-MeN cation, the vibrational structure was observed for a visible and a UV state; for naphthalene, only a UV state was observed. UV $^{+}0_0^0$ transition wavelengths for the cations occur at 304.7 nm (naphthalene) and 308.9 nm (2-MeN). Mass spectra for 2-MeN are given in Fig. 8 for resonance ion excitation at 662 nm. The H atom dissociation at this wavelength is very distinctive and specific. Only a small yield of the next lowest energy dissociation channel, loss of C_2H_2, is also evident. Ion dip spectra for naphthalene and 2-MeN cations, formed by ω_2, were recorded by scanning ω_2 for vibrationless and vibrationally excited cation.[6] The corresponding ion formation spectrum for the fragment ion $[M-1]^+$ is illustrated in Fig. 9 for naphthalene cations prepared in the 0_0 level.

The linewidths in the RID spectra of the cations are rather broad for both the visible ($\sim$200 cm^{-1}, Fig. 5) and the UV resonances ($\sim$150 cm^{-1}, Figs. 6), although they are comparable to the matrix absorption spectra.[15] However, a pronounced power broadening was evident in which the visible transitions of the cooled 2-MeN ions were saturated, even relatively far from resonance. This behavior can be explained[6] by the presence of a strong continuum background absorption to longer wavelengths, which is believed to be associated with a lower excited electronic state.

For selective detection, the broadness of the ion transitions is somewhat discouraging. However, the decreased optical selectivity in the ω_2 excitation step is compensated by the increased mass selectivity resulting from parent/fragment detection. Furthermore, the visible absorptions in the aromatic ions are very selective in that there is no overlapping absorption by neutral molecules. Finally, the dissociation process is very efficient (Fig. 8); consequently the detection efficiency is favorable by this scheme.

IV. Summary and Conclusions

Two-color multiresonant laser excitation using mass-resolved ion detection has been demonstrated to be an effective method for detecting higher excited electronic states of molecules and ions. The preparation of cold molecules in a supersonic molecular beam allows discrete vibronic resonances to be observed. These considerations account for very high detection selectivity, a condition of utmost importance to trace monitoring applications. Three excitation/detection methods have been reported. The double resonant ion dip excitation spectrum of a higher excited electronic state of aniline revealed extensive vibrational structure. Discrete absorptions were also observed above the ionization potential for naphthalene, which are attributable to autoionizing Rydberglike states. In both cases, the absorption processes are efficient and, therefore, satisfactory for trace detection purposes. Aniline was also the subject of detection by stimulated emission pumping. The detection sensitivity was examined using a density matrix model to identify the behavior of the ion dip signal in the weak and strong pulse energy limits. Finally, resonance ion dissociation was studied as a possible means of obtaining quadruply dispersive selectivity (two optical and

two mass stages). Discrete resonances in the ion were detected by monitoring the decrease of the parent M^+ signal and the corresponding increase of the fragment $[M - m]^+$ signal.

We are indebted to Larry Pruitt for valuable assistance in recording the spectra presented here. This work was supported by the Department of Energy under contract DE-FG03-ER6039.

References

1. J. W. Hager, M. A. Smith, and S. C. Wallace, "Two Color Threshold Photoionization of Jet Cooled Aniline: Vibrationally Selective Autoionization," J. Chem. Phys. **84,** 6771 (1986); M. A. Smith, J. W. Hager, and S. C. Wallace, "Two Color Photoionization Spectroscopy of Jet Cooled Aniline: Vibrational Frequencies of the Aniline $\tilde{X}^2B_1$ Radical Cation," J. Chem. Phys. **80,** 3097 (1984).
2. I. Nadler, M. Noble, H. Reisler, and C. Wittig, "The Monoenergetic Vibrational Predissociation of Expansion Cooled NCNO: Nascent CN(V,R) Distribution at Excess Energies 0–5000 cm^{-1}," J. Chem. Phys. **82,** 2608 (1985).
3. J. A. Syage and J. E. Wessel, "Ion Dip Spectroscopy of Higher Excited Vibronic States of Aniline," J. Chem. Phys. **85,** 6806 (1986).
4. J. Murakami, K. Kaya, and M. Ito, "Ion Dip Spectra of Toluene and Aniline in a Supersonic Free Jet," Chem. Phys. Lett. **91,** 401 (1982).
5. T. Suzuki, N. Mikami, and M. Ito, "Ion Dips in Two-Color Photoionization Spectra of Jet-Cooled Trans-Stilbene. Stimulated Transitions to Ground-State Vibrational Levels," Chem. Phys. Lett. **120,** 333 (1985); J. Xie, G. Sha, X. Zhang, and C. Zhang, "Ion Dip Spectroscopy as a Means of Probing Fast Predissociating Species: NH_3 $\tilde{A}^1A_2''$ State," Chem. Phys. Lett. **124,** 99 (1986).
6. J. A. Syage and J. E. Wessel, "Resonance Ion Dissociation Spectroscopy of Naphthalene Ions Prepared in a Supersonic Expansion," J. Chem. Phys. **87,** (1987).
7. J. A. Syage and J. E. Wessel, "Antiresonance in Autoionizing Rydberg Series of Naphthalene," J. Chem. Phys., submitted.
8. D. M. Lubman and R. M. Jordan, "Design for Improved Resolution in a Time-of-Flight Mass Spectrometer using a Supersonic Beam and Laser Ionization Source," Rev. Sci. Instrum. **56,** 373 (1985); U. Boesl, H. J. Neusser, and E. W. Schlag," Multi-Photon Ionization in the Mass Spectrometry of Polyatomic Molecules: Cross Sections," Chem. Phys. **55,** 193 (1981).
9. J. A. Syage, J. E. Pollard, and R. B. Cohen, "Ultrasensitive Detection of Atmospheric Constituents by Supersonic Molecular Beam, Multiphoton Ionization, Mass Spectroscopy," Appl. Opt. **26,** 000 (1 Sept. 1987).
10. D. H. Levy, L. Wharton, and R. E. Smalley, in *Chemical and Biological Applications of Lasers, Vol. 2* (Academic, New York, 1977), p. 1.
11. D. E. Cooper, C. M. Klimcak, and J. E. Wessel, "Ion Dip Spectroscopy: A New Technique of Multiphoton Ionization Spectroscopy Applied to I_2," Phys. Rev. Lett. **46,** 324 (1981); D. E. Cooper and J. E. Wessel, "Identification of a High Energy State of I_2 by Ion Dip Spectroscopy," J. Chem. Phys. **76,** 2155 (1982).
12. D. J. Moll, G. R. Parker, and A. Kuppermann, "Time-Resolved Two-Color Photoacoustic and Multiphoton Ionization Spectroscopy of Aniline," J. Chem. Phys. **80,** 4808 (1984).
13. K. F. Freed, "Radiationless Transitions in Molecules," Acc. Chem. Res. **11,** 74 (1978).
14. J. R. Ackerhalt and B. W. Shore, "Rate Equations versus Bloch Equations in Multiphoton Ionization," Phys. Rev. A **16,** 277 (1977).
15. L. Andrews, B. J. Kelsall, and T. A. Blankenship, "Vibronic Absorption Spectra of Naphthalene and Substituted Naphthalene Cations in Solid Argon," J. Phys. Chem. **86,** 2916 (1982).
16. J. P. Honovich, J. Segall, and R. C. Dunbar, "Fragmentation Thermochemistry of Gas-Phase Ions by Threshold Photodissociation and Charge-Exchange Ionization. Methylnaphthalene and Methylstyrene Ions," J. Phys. Chem. **89,** 3617 (1985); M. S. Kim and R. C. Dunbar, "Naphthalene Ion Photodissociation: Two- and Four-Photon Processes," J. Chem. Phys. **72,** 4405 (1980).
17. D. Mordaunt, G. Loper, and J. Wessel, "Multiphoton Ionization-Fragmentation Spectroscopy of Methylnaphthalenes," J. Phys. Chem. **88,** 5197 (1984).